HNUE JOURNAL OF SCIENCE
Natural Sciences 2025, Volume 70, Issue 2, pp. 111-119
This paper is available online at http://hnuejs.edu.vn/ns
DOI: 10.18173/2354-1059.2025-0026

STRUCTURE AND LUMINESCENCE OF $Bi_2Zr_2O_7:Eu^{3+},Tb^{3+}$ RED PHOSPHORS FOR WHITE LIGHT-EMITTING DIODES

Nguyen Van Hai[1,*], Vu Thi Ngoc Linh[1], Ho Van Cuu[2] and Nguyen Viet Long[2]
[1]*Faculty of Chemistry, Hanoi National University of Education, Hanoi city, Vietnam*
[2]*FET Faculty of Engineering and Technology, Sai Gon University, Ho Chi Minh city, Vietnam*
[*]Corresponding author: Nguyen Van Hai, e-mail: hainv@hnue.edu.vn

Received April 9, 2025. Revised May 27, 2025. Accepted June 30, 2025.

Abstract. In this study, Eu^{3+} and Tb^{3+} co-doped $Bi_2Zr_2O_7$ (BZO) pyrochlore phosphors were successfully synthesized via a combustion method at 600 °C. The crystal structure, elemental composition, morphology, luminescent characteristics, and energy transfer behavior were systematically investigated. Powder X-ray diffraction (XRD) analysis confirmed that all synthesized samples exhibited a pure single-phase pyrochlore structure, with Eu^{3+} and Tb^{3+} ions efficiently incorporated into the host lattice. Under blue light excitation at 466 nm, BZO:Eu^{3+},Tb^{3+} phosphors exhibited relatively strong red emission. Efficient energy transfer from Tb^{3+} to Eu^{3+} was observed, leading to a significant enhancement in red luminescence. Furthermore, the obtained phosphors demonstrated color purities approaching 90%. These results suggest that Tb^{3+} ions effectively act as sensitizers to Eu^{3+}, and the new kinds of BZO:Eu^{3+},Tb^{3+} phosphors hold great potential for application in blue-excited white light-emitting diodes (WLEDs).

Keywords: $Bi_2Zr_2O_7$, energy transfer, Eu^{3+} and Tb^{3+}, luminescence, red phosphor.

1. Introduction

In recent years, white light-emitting diodes (WLEDs) have emerged as a promising solid-state lighting technology, offering a viable alternative to conventional fluorescent and incandescent light sources. WLEDs possess several key advantages, including high luminous efficacy, low power consumption, and environmental sustainability, which have driven their widespread adoption in various applications [1], [2]. The most commonly used commercial WLEDs are typically fabricated by integrating a yellow-emitting phosphor, $Y_3Al_5O_{12}:Ce^{3+}$ (YAG:Ce^{3+}), dispersed in a silicon matrix and deposited onto a blue InGaN chip. Despite the simplicity and efficiency of this

configuration, it suffers from inherent limitations, notably a low color rendering index (CRI) and a high correlated color temperature (CCT), primarily due to the lack of sufficient red spectral components. To overcome these deficiencies, Eu^{3+}-activated red-emitting phosphors have attracted significant attention as effective candidates for enhancing the red component in phosphor-converted WLED systems [3]-[5]. Therefore, the development of highly efficient red-emitting phosphors is essential to advance color quality and overall performance of next-generation WLEDs.

Trivalent europium ion (Eu^{3+}) is widely recognized as one of the most commonly utilized red-emitting activators. The characteristic red emissions of Eu^{3+} originate from magnetic dipole ($^5D_0$–$^7F_1$) and electric dipole ($^5D_0$–$^7F_2$) transitions, both of which are strongly influenced by the crystal field symmetry of the host lattice. To date, Eu^{3+} ions have been extensively doped into various host matrices, including silicates, titanates, fluorides, aluminosilicates, oxysulfides, and metal oxides [6]. In order to enhance the red emission efficiency of Eu^{3+}, the incorporation of sensitizer ions via energy transfer mechanisms has been proven to be particularly effective.

Tb^{3+} ion is recognized as a green-emitting luminescent center, primarily due to its 4f → 4f transitions. Moreover, owing to the similarity in energy levels between Tb^{3+} and Eu^{3+} ions, efficient energy transfer from Tb^{3+} to Eu^{3+} can be achieved. Consequently, co-doping with Tb^{3+} and Eu^{3+} has facilitated the development of various multicolor-tunable phosphor materials [7]. These phosphors have garnered considerable attention due to their promising applications in solid-state lighting and multicolor display technologies. To date, several Tb^{3+}/Eu^{3+} co-doped phosphors based on different host matrices have been reported, including $LaPO_4$ [8], $KBaIn_2(PO_4)_3$ [9], $Al_2(WO_4)_3$:Eu,Tb [10], phosphate glass [11], and various kinds of borosilicate glass [12].

Recently, zirconate materials with the general formula $A_2Zr_2O_7$ have been extensively investigated for applications in solid-state lighting, sensing, and cellular imaging [13], [14]. Typically, $A_2Zr_2O_7$ adopts a pyrochlore structure with the space group *Fd-3m*, provided that the ionic radius ratio lies within the range of $1.46 \leq r(A^{3+})/r(Zr^{4+}) \geq 1.78$ [14]. When A is Bi, the resulting BZO crystal is also characterized by a stable pyrochlore structure, in which Bi^{3+} and Zr^{4+} cations are coordinated by eight and six oxygen atoms, respectively.

Although numerous studies have demonstrated that Eu^{3+}/Tb^{3+} co-doped materials are promising candidates for solid-state lighting applications, to the best of our knowledge, the luminescent properties of the BZO:Eu^{3+},Tb^{3+} system have not yet been reported.

In the present study, BZO:Eu^{3+},Tb^{3+} (0- 6 mol%) nanophosphors were successfully synthesized via a combustion method. Subsequently, the photoluminescence properties of the obtained samples were systematically investigated and analyzed to assess their potential applicability in WLEDs.

2. Content

2.1. Experimental

2.1.1. Materials and synthesis

A series of BZO:Eu^{3+},Tb^{3+} phosphors were synthesized via a combustion reaction method. Specifically, $Bi(NO_3)_3 \cdot 5H_2O$, $ZrOCl_2 \cdot 8H_2O$, Tb_4O_7, and Eu_2O_3, all with a purity of 99.5%, were used without further purification. $ZrOCl_2 \cdot 8H_2O$ was first converted into $ZrO(NO_3)_2$ by reacting with an excess amount of concentrated HNO_3, followed by evaporation of the solvent to remove residual water and nitric acid. Similarly, Tb_4O_7 and Eu_2O_3 were converted into $Tb(NO_3)_3$ and $Eu(NO_3)_3$, respectively, by dissolving them in concentrated HNO_3 and heating the solution. The nitrate solutions of Bi^{3+}, Zr^{4+}, Eu^{3+}, and Tb^{3+} were subsequently mixed in a molar ratio of (196 - x):200:4:x, where *x* denotes the molar doping concentration of Tb^{3+}. The resulting mixture was continuously stirred at 80 °C until a viscous precursor was formed. The precursor was then subjected to calcination at 400 °C for 4 h, followed by cooling and grinding. A subsequent annealing step was carried out at 600 °C for 4 h with a heating rate of 10 °C/min to yield the final BZO:Eu^{3+},Tb^{3+} phosphor powders.

2.1.2. Methodology

D8-Advance diffractometer with Cu Kα radiation (λ = 0.015405 nm). The surface morphology of the phosphor samples was observed via scanning electron microscopy (SEM) using a HITACHI S-4800 instrument. Elemental composition analysis was performed using energy-dispersive X-ray spectroscopy (EDX) equipped with a HORIBA 7593-H detector attached to an FESEM system.

Diffuse reflectance spectra (DRS) were measured using a JASCO 670 spectrophotometer over the wavelength range of 250 - 800 nm. The photoluminescence excitation and emission spectra were recorded using a Horiba Jobin Yvon Nanolog spectrometer equipped with a 450 W xenon (Xe) lamp, operating in the wavelength range of 350 - 750 nm. All characterization experiments were conducted at room temperature.

2.2. Results and discussion

2.2.1. Structure, composition, and morphology of phosphors

To determine the crystal structure and phase purity, the XRD patterns of BZO, BZO:Eu^{3+}, and BZO:Eu^{3+},Tb^{3+} samples were recorded, as shown in Figure 1. The diffraction peaks of all samples were found to be in good agreement with the standard pyrochlore phase of BZO, as previously reported in the literature [13], [14]. No secondary phases such as Bi_2O_3 or ZrO_2 were detected in the diffraction patterns, indicating that the synthesized materials are phase-pure. Furthermore, it can be inferred that the co-doping of Eu^{3+} and Tb^{3+} ions was successfully incorporated into the host lattice without altering the single-phase pyrochlore structure. On the other hand, the annealing temperature in this study is 600 °C, which is lower than that employed for the

$Bi_2Zr_2O_7$:Er,Yb phosphor synthesized using urea or thiourea as fuel, where annealing was carried out at temperatures ranging from 775 to 850 ºC [14].

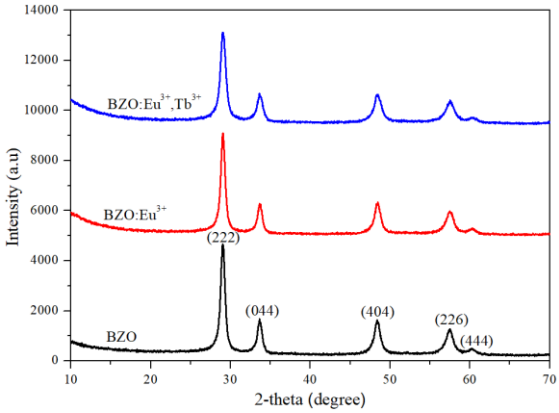

Figure 1. XRD pattern of BZO, BZO:Eu^{3+}, and BZO:Eu^{3+},Tb^{3+} materials annealed at 600 °C

Based on the XRD data, the average crystallite size was estimated using Debye–Scherrer equation, $D = \frac{K\lambda}{\beta\cos\theta}$, where D is the crystallite size, K is the shape factor (typically 0.9), λ is the wavelength of the X-ray source, β is the full width at half maximum (FWHM) of the diffraction peak, and θ is the Bragg angle.

Table 1. The average crystal size of BZO:4%Eu^{3+},xTb^{3+} (x = 0, 2, 4, 6)

Phosphors	B (rad)	2θ (degree)	D (nm)
BZO	0.0129	29.05	34.5
BZO:4%Eu^{3+},2%Tb^{3+}	0.0202	29.29	24.4
BZO:4%Eu^{3+},4%Tb^{3+}	0.0238	29.25	21.8
BZO:4%Eu^{3+},6%Tb^{3+}	0.0238	29.33	20.7

To determine the elemental composition of Eu-Tb co-doped BZO, the energy dispersive X-ray (EDX) spectrum of BZO:4%Eu^{3+},4%Tb^{3+} phosphor was recorded, as presented in Figure 2.

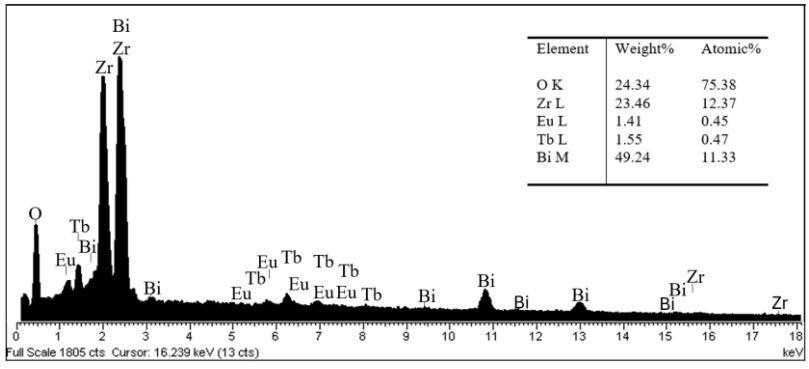

Figure 2. EDX spectrum of the BZO:4%Eu^{3+},4%Tb^{3+} phosphor

In Figure 2, all constituent elements are identified in the material without any detectable impurities. Furthermore, atomic ratios of metal elements are found to be approximately consistent with the stoichiometric composition of the material.

To investigate the photon absorption capability of the as-prepared material, diffuse reflectance spectra (DRS) were recorded to determine band gap energy, as shown in Figure 3.

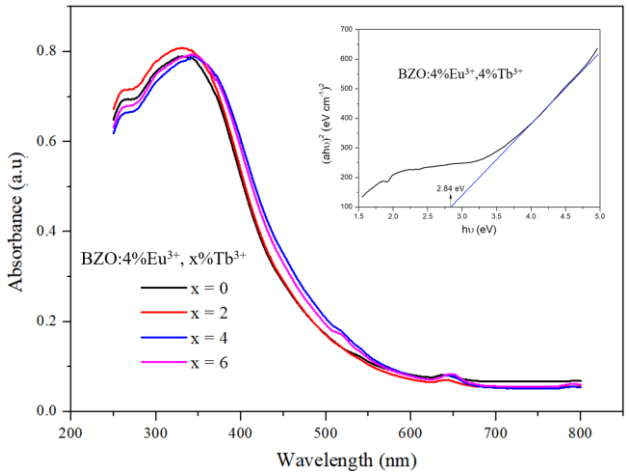

Figure 3. The DRS of the BZO:4%Eu^{3+},x%Tb^{3+} materials and the Tauc plot of the BZO: 4%Eu^{3+},4%Tb^{3+} sample (the inset)

The results presented in Figure 3 indicate that the BZO:4%Eu^{3+},x%Tb^{3+} material exhibits strong absorption in the near-ultraviolet and green regions of the spectrum. Furthermore, the band gap energy (E_g) of the BZO:4%Eu^{3+},4%Tb^{3+} phosphor was determined to be 2.84 eV, corresponding to an excitation wavelength of 436 nm. The value of E_g is higher than the reported range of 2.63-2.67 eV in reference [13].

The SEM image of the BZO:4%Eu^{3+},4%Tb^{3+} sample is shown in Figure 4. The material particles are observed to possess a cuboid-like morphology, with particle sizes varying over a wide distribution range.

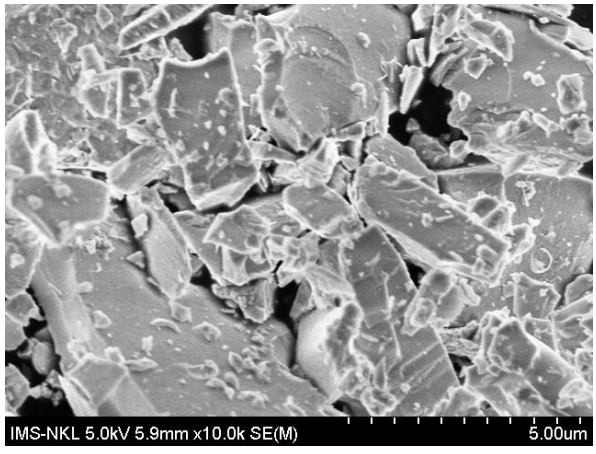

Figure 4. SEM image of the BZO:Eu^{3+},Tb^{3+} phosphor

2.2.2. Fluorescent properties of the phosphors

**** Photoluminescence excitation spectra***

To determine the appropriate excitation wavelength for the BZO:4%Eu^{3+}, x%Tb^{3+} (x = 0, 2, 4, 6, 8) material, the fluorescence excitation spectrum corresponding to the red emission peaks at 591 nm ($^5D_0$–$^7F_1$) and 608 nm ($^5D_0$–$^7F_2$) of Eu^{3+} was recorded, as shown in Figure 5.

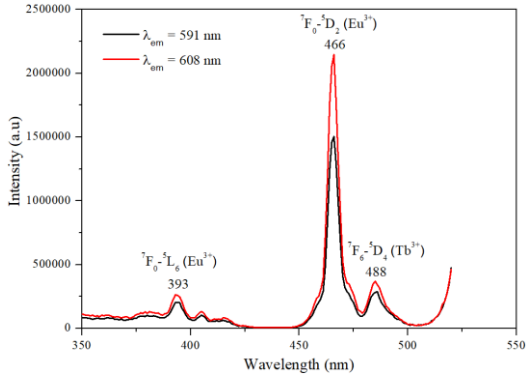

Figure 5. Fluorescence excitation spectra of BZO:4%Eu^{3+},4%Tb^{3+} phosphor

As shown in Figure 5, the emission intensities at 591 nm ($^5D_0$–$^7F_1$) and 608 ($^5D_0$–$^7F_2$) of Eu^{3+} are the strongest when excited at a wavelength of 466 nm. This result suggests that the synthesized phosphor can emit intense red light under blue LED excitation (440 - 470 nm), thereby effectively enhancing the red component in the fabrication of WLEDs.

**** Photoluminescence emission spectra***

Based on the fluorescence excitation spectrum, the fluorescence emission spectra of the BZO:4%Eu^{3+},x%Tb^{3+} (x = 0, 2, 4, 6) phosphors were recorded under an excitation wavelength of 466 nm, as shown in Figure 6.

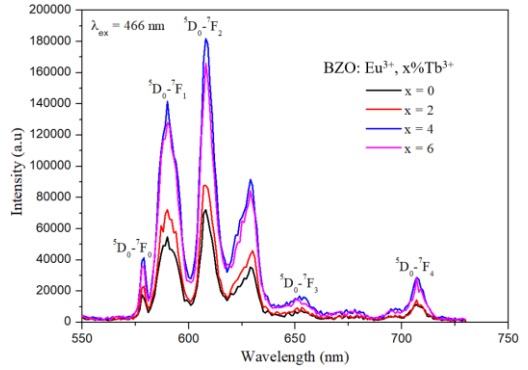

Figure 6. Photoluminescence emission spectra of BZO:Eu^{3+},Tb^{3+} products with different Tb^{3+} concentrations

Figure 6 shows the characteristic fluorescence peaks of Eu^{3+}, including $^5D_0$-$^7F_0$ (578 nm), $^5D_0$-$^7F_1$ (591 nm), $^5D_0$-$^7F_2$ (608 nm), $^5D_0$-$^7F_3$ (653 nm), and $^5D_0$-$^7F_4$ (703 nm). Among these, the two intense red emission peaks $^5D_0$-$^7F_1$ and $^5D_0$-$^7F_2$ were particularly

prominent. Furthermore, the fluorescence intensity was significantly enhanced by Tb^{3+} doping, with the maximum intensity observed at a Tb^{3+} concentration of 4%. The corresponding energy levels and energy transfer mechanism from Tb^{3+} to Eu^{3+} are schematically illustrated in Figure 7.

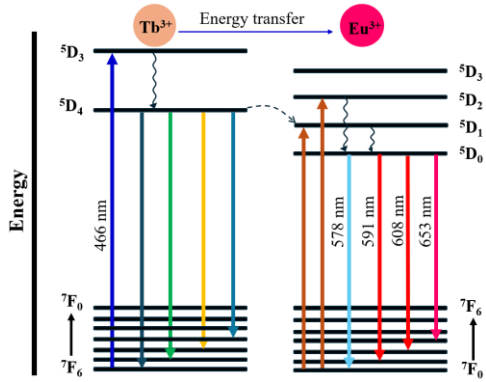

Figure 7. Energy level diagram of Tb^{3+} and Eu^{3+} and the energy transfer process in the BZO:Eu^{3+},Tb^{3+} phosphor

As illustrated in Figure 7, under 466 nm excitation, Tb^{3+} ions were initially excited from the ground state $^7F_6$ to the higher-energy $^5D_3$ excited state. Subsequently, a portion of these ions was non-radiatively relaxed to the energetically lower $^5D_4$ level. At this state, energy was transferred from Tb^{3+} ions to the $^5D_1$ level of Eu^{3+} ions, owing to the proximity of their energy levels. Thereafter, the Eu^{3+} ions were further relaxed to the $^5D_0$ level, followed by a series of radiative transitions $^5D_0$-^7F_J (J = 0, 1, 2, 3, 4), corresponding to the emission wavelengths of 578 nm, 591 nm, 608 nm, 653 nm, and 703 nm, respectively. In parallel, Tb^{3+} ions remaining in the $^5D_4$ level decayed radiatively to the lower-lying ^7F_J states (J = 6, 5, 4, 3), resulting in green emissions. However, the emission peaks of Tb^{3+} were comparatively weaker than those of Eu^{3+} ions, and were thus partially overshadowed by the stronger Eu^{3+} emissions. Furthermore, the chromaticity coordinates based on the International Commission on Illumination (CIE) system were calculated from the measured emission spectra, as shown in Figure 8.

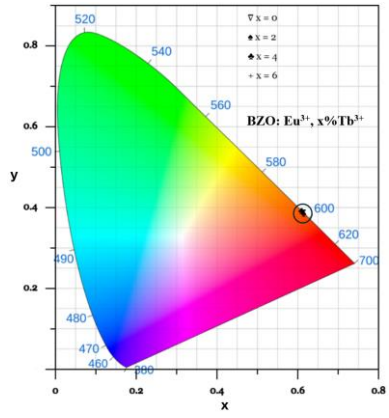

Figure 8. Color coordinates of the BZO:4%Eu^{3+},x%Tb^{3+} samples

According to Figure 8, as the concentration of Tb^{3+} increased, the color of the BZO:4%Eu^{3+},x%Tb^{3+} phosphors remained predominantly red, corresponding to the Eu^{3+} emission center, without exhibiting any significant shift toward the green emission associated with Tb^{3+} ions. This observation further confirms the efficient energy transfer from Tb^{3+} to Eu^{3+}. Consequently, the emission peaks of Tb^{3+} were gradually quenched, while those of Eu^{3+} were enhanced, resulting in red emission being dominant over green emission. Moreover, the chromaticity coordinates, CCT, and color purity were calculated from the corresponding emission spectra, as summarized in Table 2.

Table 2. The corresponding chromaticity of selected BZO:Eu^{3+},Tb^{3+} phosphors

Samples	Color coordinates	Color purity	CCT (K)
BZO:4%Eu^{3+}	(0.613; 0.386)	88.87	1774.2
BZO:4%Eu^{3+},2%Tb^{3+}	(0.615; 0.384)	89.30	1791.6
BZO:4%Eu^{3+},4%Tb^{3+}	(0.608; 0.391)	87.81	1740.6
BZO:4%Eu^{3+},6%Tb^{3+}	(0.610; 0.389)	88.23	1750.0

The results in Table 2 show that the BZO:4%Eu^{3+},x%Tb^{3+} phosphors emit red light with high color purity and chromaticity coordinates comparable to those of $LiYF_4$:28%Tb^{3+}/8.5Eu^{3+} [1], $Ca_8MgTb_{1-y}(PO_4)_7$:0.7Eu^{3+} [3], and $Ba_{1.94}P_2O_7$:0.06Eu^{3+} [4], despite the use of lower doping concentrations. This suggests that these materials are promising luminescent candidates for enhancing the red component in the fabrication of WLEDs.

3. Conclusions

In summary, BZO:Eu^{3+},Tb^{3+} phosphors with a pyrochlore structure were successfully synthesized via a combustion method at 600 °C. Under excitation at 466 nm, strong red emissions were observed, corresponding to the $^5D_0 \rightarrow {}^7F_1$ and $^5D_0 \rightarrow {}^7F_2$ transitions of Eu^{3+} ions. Tb^{3+} ions effectively served as sensitizers, facilitating energy transfer from the $^5D_4$ level of Tb^{3+} to the $^5D_1$ level of Eu^{3+}, thereby enhancing the overall luminescence. The optimal doping concentration of Tb^{3+} was determined to be 4 mol%. Furthermore, the high color purity exhibited by BZO:Eu^{3+},Tb^{3+} phosphors indicates their promising potential for improving the red emission component in WLEDs applications.

REFERENCES

[1] D, Jorge M-G, Octavio M, Priscilla C & Juan B-P, (2019). Multicolor and Warm White Emissions with a High Color Rendering Index in a Tb^{3+}/Eu^{3+}-Codoped Phosphor Ceramic Plate. *Materials*, 12, 2240; DOI: 10.3390/ma12142240.

[2] Vijayalakshmi L, Naveen K & Pyung H, (2020). Tailoring ultraviolet-green to white light via energy transfer from Tb^{3+} - Eu^{3+} codoped glasses for white light-emitting diodes. *Scripta Materialia* 187, 97-102. DOI: 10.1016/j.scriptamat.2020.06.014.

[3] Feiyan X, Junhao L, Zhiyue D, Dawei W, Jianxin S, Jing Y & Mingmei W, (2015). Energy transfer and luminescent properties of $Ca_8MgLu(PO_4)_7$:Tb^{3+}/Eu^{3+} as a

green-to-red color tunable phosphor under NUV excitation. *RSC Advances*., 5, 59830. DOI: 10.1039/c5ra08680a.

[4] Baoxing W, Qiang R, Ou H & Xiulan W, (2017). Luminescence properties and energy transfer in Tb^{3+} and Eu^{3+} co-doped $Ba_2P_2O_7$ phosphors. *RSC Advances*, 7, 15222. DOI: 10.1039/c6ra28122b.

[5] Nimai P, Bhagyalaxmi C, Pratik D, Pampa M & Brindaban M, (2021). Unraveling the site-specific energy transfer driven tunable emission characteristics of Eu^{3+} & Tb^{3+} codoped $Ca_{10}(PO_4)_6F_2$ phosphors. *RSC Advances*, 11, 31421. DOI: 10.1039/d1ra04941k.

[6] He Z, Benfu Q, Xiuqing Z, Yanhua S, Keyan Z, Ye S & Haifeng Z, (2018). Tuneable luminescence and energy transfer of Tb^{3+}/Eu^{3+} co-doped cubic $CaCO_3$ nanoparticles. *Journal of Luminescence*, 203, 441-446. DOI: 10.1016/j.jlumin.2018.06.041.

[7] Zhipeng F, Yaqin Q, Dengkui G, Yixuan L, Fanqi K, Zhan S & Hua Y, (2021). Multicolor tunable emission and energy transfer in AlN:Tb^{3+},Eu^{3+} phosphors. *Journal of Materials Science: Mater Electron* 32, 210-218. DOI: 10.1007/s10854-020-04756-y.

[8] Yuxia L, Zhenyu L, Hon TW, Lei Z, Ka-Leung W, Kwok KS & Peter AT, (2019). Energy Transfer between Tb^{3+} and Eu^{3+} in $LaPO_4$: Pulsed versus Switched-off Continuous Wave Excitation. *Advance Science*, 1900487. DOI: 10.1002/advs.201900487.

[9] Xu MJ, Si JY, Li GH, Liu YJ, Cai GM & Zhang J, (2020). Structure, tunable luminescence and thermal stability in Tb^{3+} and Eu^{3+} co-doped novel $KBaIn_2(PO_4)_3$ phosphors. *Journal of Luminescence* 221, 117115. DOI: 10.1016/j.jlumin.2020.117115.

[10] Ziqian L & et al, (2024). Achieving zero-thermal quenching of $Al_2(WO_4)_3$:Eu,Tb red phosphors with low thermal expansion for LEDs. *Ceramics International*. 50(18B), 33217-33224. DOI: 10.1016/j.ceramint.2024.06.132.

[11] Nihel H, Chaker B, (2022). White luminescence and energy transfer studies in Tb^{3+}-Eu^{3+} co-doped phosphate glasses. *Solid State Sciences* 134, 107053. DOI: 10.1016/j.solidstatesciences.2022.107053.

[12] Hong J & et al, (2024). Fabrication of Tb/Eu co-doped borosilicate glasses for white-light LED and broadband photodetection. *Journal of Rare Earths*. DOI: 10.1016/j.jre.2024.06.003.

[13] Rajashekharaiah AS & et al, (2019). NUV light-induced visible green emissions of Erbium-doped hierarchical $Bi_2Zr_2O_7$ structures. *Optical Materials* 95, 109237. DOI: 10.1016/j.optmat.2019.109237.

[14] Rosales M, Oliva J, Desirena H & Salas P, (2024). Effect of Urea and Thiourea on the color emission of $(Y_xBi_{1-x})_2Zr_2O_7:Er^{3+},Yb^{3+}$ upconversion phosphors. *Optical Materials* 157, 116307. DOI: 10.1016/j.optmat.2024.116307.